

# Flow-Modulated Scoring for Semantic-Aware Knowledge Graph Completion

Siyuan Li\*

yuanlsy@mail.dlut.edu.com  
Dalian University of Technology  
School of Computer Science and Technology  
Dalian, China

Yan Wen

Beijing Institute of Technology School of Mechanical  
School of Engineering  
Beijing, China

Ruitong Liu†

Dalian University of Technology  
Faculty of Mathematical Sciences  
Dalian, China

Te sun

Dalian University of Technology  
School of Control Science and Engineering  
Dalian, China

## Abstract

Effective modeling of multifaceted relations is pivotal for Knowledge Graph Completion (KGC). However, a majority of existing approaches are predicated on static, embedding-based scoring, exhibiting inherent limitations in capturing contextual dependencies and relational dynamics. Addressing this gap, we propose the Flow-Modulated Scoring (FMS) framework. FMS comprises two principal components: (1) a semantic context learning module that encodes context-sensitive entity representations, and (2) a conditional flow-matching module designed to learn the dynamic transformation from a head to a tail embedding, governed by the aforementioned context. The resultant predictive vector field, representing the context-informed relational path, serves to dynamically refine the initial static score of an entity pair. Through this synergy of context-aware static representations and conditioned dynamic information, FMS facilitates a more profound modeling of relational semantics. Comprehensive evaluations on several standard benchmarks demonstrate that our proposed method surpasses prior state-of-the-art results.

## CCS Concepts

• **Computing methodologies** → **Knowledge representation and reasoning**; **Machine learning**.

## Keywords

Knowledge graph, Graph embedding, Knowledge graph completion, Diffusion model, Graph representation learning, Graph neural network

## 1 Introduction

Knowledge graphs (KGs) serve as a powerful tool for knowledge representation, utilizing entity nodes and directed edges to describe entities and their interrelations in the real world. Each knowledge graph is typically composed of a large number of triples  $(h, r, t)$ , where each triple precisely delineates how a head entity  $h$  is associated with a tail entity  $t$  through a specific relation  $r$ . Due to their exceptional ability to efficiently organize and represent complex semantic facts, knowledge graphs have become a cornerstone in the

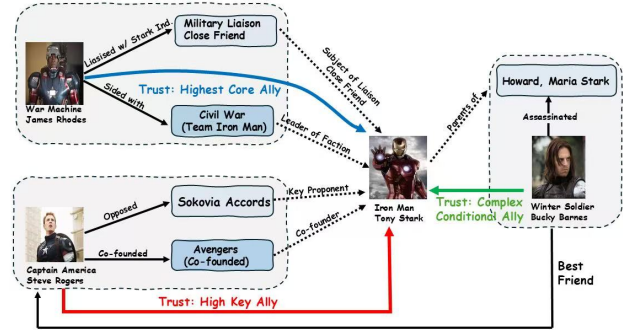


**Figure 1:** This figure systematically depicts the dynamic interplay of Iron Man’s relationships with War Machine, Captain America, and the Winter Soldier, all broadly defined as allies. However, the specific semantics of these alliances exhibit varying degrees, which are profoundly shaped by the semantic context—namely, distinct historical junctures, critical incidents, and individual value perspectives.

field of artificial intelligence, playing a pivotal role in large-scale applications such as recommender systems, information extraction, and intelligent question answering [9, 22, 40].

However, due to the continuous evolution of knowledge and the high cost and complexity of knowledge acquisition, real-world knowledge graphs, despite their vast scale, often suffer from incomplete or missing information. This limitation partially undermines their application efficacy and knowledge inference capabilities. To address this challenge, the task of Knowledge Graph Completion (KGC) has emerged, aiming to infer and predict missing links based on existing facts.

Relation Prediction (RP) between entity pairs stands as one of the pivotal sub-tasks within Knowledge Graph Completion. Specifically, given a head entity  $h$  and a tail entity  $t$ , the RP task aims to learn a function  $f(\cdot)$  that predicts a set of plausible relations  $\mathcal{R}$  between them, formally denoted as  $f(h, t) = \mathcal{R}$ . To address this, researchers have explored a multitude of methodologies. Initially, embedding-based models, such as TransE [2], were pioneered. These models

\*Corresponding author.

†Both authors contributed equally to this research.

conceptualize relations as translation vectors from the head entity to the tail entity, evaluating the plausibility of a triplet via simple vector operations. Despite their conciseness and efficiency, such methods often struggle to effectively handle complex relational patterns, including one-to-many, many-to-one, and many-to-many scenarios. To overcome these limitations, subsequent works such as TransH [41], TransR [16] and TransD [10] significantly improved the modeling capacity for complex relations by introducing relation-specific projection hyperplanes or mapping matrices. Concurrently, another line of research has focused on leveraging more sophisticated semantic matching architectures. For instance, models based on multilinear interactions such as DistMult [42], and ComplEx [36], aim to capture deeper and richer interaction patterns between entities and relations by designing more elaborate scoring functions. While these embedding-based methods have achieved considerable progress in KGC tasks, their core paradigm predominantly relies on learned static embeddings for entities and relations, employing a fixed scoring function to assess the confidence of triplets. This paradigm may, to some extent, fall short in fully capturing the subtle semantic nuances of relations across diverse contexts and the dynamic evolutionary characteristics of inter-entity relationships, thereby potentially limiting their representational power and predictive accuracy. Taking the relationships among Marvel characters as an example (see the Figure 1), in a work-related context, Iron Man and War Machine share a military liaison relationship, with War Machine acting as Iron Man’s supporter, making them core allies. Iron Man and Captain America are co-founders of the Avengers but hold opposing views on the Sokovia Accords; overall, they remain key allies. In contrast, the Winter Soldier, despite being Captain America’s best friend, assassinated Iron Man’s parents, resulting in a complex ally relationship with Iron Man. Clearly, these characters’ relationships vary across semantic contexts, with differing degrees of closeness. Notably, during reasoning, the semantic contexts we rely on are more about relational attributes than entity attributes.

Since then, GNN-based methods have gradually emerged. For instance, in the RP task, the most representative method, PathCon [39], models the probability distribution of relations by incorporating the context and multi-hop paths of entity pairs to achieve prediction. However, like other GNN-based methods, this approach is constrained by static context, thus failing to effectively handle the dynamic nature of relations.

Recently, inspired by the strong semantic comprehension of large language models (LLMs), LLM-based approaches have been increasingly applied to relation prediction tasks. For instance, KG-BERT [44] converts knowledge graph triples into textual sequences, leveraging BERT’s semantic encoding for relation prediction. Nadkarni et al. [20] employ a BERT model fine-tuned for the biomedical domain to effectively capture complex relational patterns among biomedical entities. Similarly, Nassiri et al. [21] introduce a triplet BERT-network model, enhancing relation prediction accuracy through semantic refinement. While these methods have shown notable advances in discerning subtle semantic nuances of relations across diverse contexts, they fail to explicitly model the dynamic evolution of inter-entity relationships. Furthermore, the large parameter scale of LLMs can hinder inference efficiency, increase deployment costs, and limit adaptability to domain-specific knowledge graphs. To address all these challenges, we propose the Flow-Modulated

Scoring (FMS) framework. This framework integrates a semantic context learning module to encode context-aware embeddings and employs a condition flow-matching module to model dynamic transformations between head and tail entities. By generating a context-driven predictive vector field, FMS dynamically adjusts static scores, thereby achieving more comprehensive and precise modeling of relation semantics across diverse contexts. Our contributions can be summarized as follows:

- We propose the Flow-Modulated Scoring (FMS) framework for knowledge graph completion, which synergizes context-aware embeddings with dynamic relation modeling, offering superior expressiveness and accuracy compared to static embedding-based methods;
- We develop a semantic context learning module that approximates semantic similarity via an energy function, selectively aggregating the Top-k relation contexts from randomly sampled candidates to construct expressive entity representations;
- We introduce a condition flow-matching module that learns a dynamic vector field to model the transformation from head to tail entity embeddings, employing Brownian Bridge Matching to capture both deterministic and stochastic relational dynamics;
- We demonstrate through comprehensive experiments that FMS achieves state-of-the-art performance across all datasets, validating its robustness in capturing dynamic relation semantics and superiority in parameter.

## 2 Related Works

### 2.1 Knowledge Graph Completion

Knowledge Graphs provide structured information for downstream tasks like recommender systems and semantic analysis. Knowledge Graph Completion, particularly Relation Prediction (RP), addresses incomplete KGs by predicting missing links. Most KGC methods rely on embedding-based approaches, which assign vectors to entities and relations in a continuous space, trained on observed facts, such as TransE [2], treat entities as points and relations as translations, aiming to position the translated head entity close to the tail entity in real, complex, or quaternion spaces. These methods effectively handle multiple relation patterns and achieve strong results. Alternatively, bilinear models like DistMult [42] and ComplEx [36] compute semantic similarity via matrix or vector dot products. Some methods explore advanced architectures beyond point vectors, such as CNN-based models [6]. However, these embedding-based approaches struggle with inductive settings. Graph Neural Network GNN-based methods, like PathCon [39], incorporate relation contexts and multi-hop paths but often neglect semantic consistency and dynamic relation modeling. Our work proposes a dynamic, context-aware framework to overcome these limitations.

### 2.2 Diffusion Models

Diffusion models, inspired by non-equilibrium thermodynamics, have achieved remarkable success in fields such as computer vision [14], sequence modeling [15, 32], and audio processing [3, 13]. Predominant approaches include Denoising Diffusion Probabilistic Models (DDPMs) [8] and Score-based Generative Models

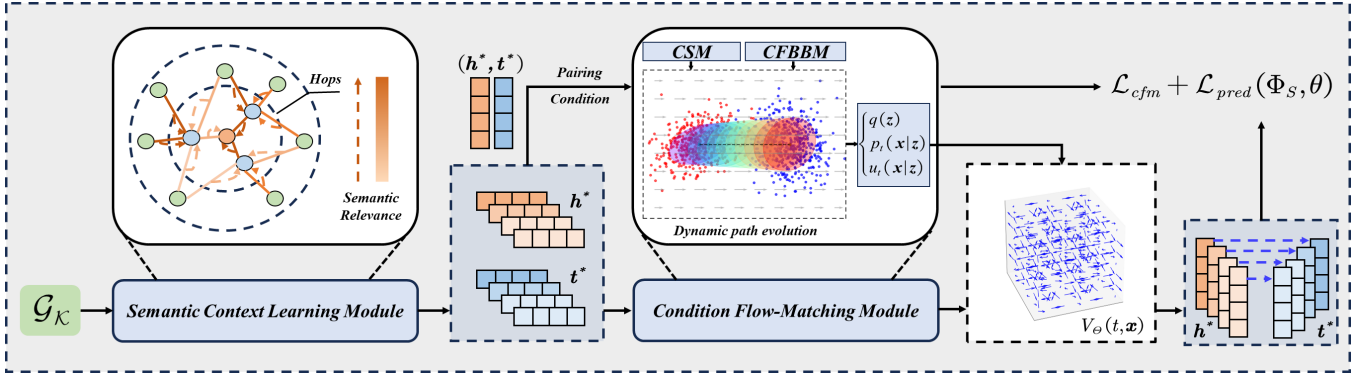


Figure 2: The FMS architecture.

(SGMs) [30]. SGMs utilize Stochastic Differential Equations (SDEs) for generation, and DDPMs can be considered an instance of SGMs under specific discretization schemes. Meanwhile, Continuous Normalizing Flows (CNFs) [5] are another attractive class of generative modeling techniques, learning an invertible mapping between the data distribution and a simple prior distribution via neural network-parameterized Ordinary Differential Equations (ODEs). Recently, research has shown that CNFs can also be trained using a regression objective similar to those in diffusion models, a method known as Flow Matching (FM) [1, 17, 18]. FM learns the transformation by directly regressing the ODE’s vector field (drift term), which is analogous to how diffusion models train score functions. The advent of FM introduced new ideas for CNF training and improved sample quality, though early FM methods typically assumed a Gaussian source distribution, a limitation addressed in subsequent work [4, 24]. Against this backdrop, Condition Flow-Matching (CFM) [34] was proposed as a generalization of FM models. CFM aims to provide a unified, simulation-free training framework for FM models with arbitrary transport maps. It inherits the stability of regression objectives from diffusion models while striving for efficient inference of deterministic flow models. Unlike traditional diffusion models and early CNF training algorithms, CFM does not require the source distribution to be Gaussian, nor does it need to evaluate its probability density.

### 3 Methodology

#### 3.1 Preliminaries

Let  $\mathcal{G} = (\mathcal{V}, \mathcal{E})$  be an instance of a knowledge graph, where  $\mathcal{V}$  is the set of entity nodes and  $\mathcal{E}$  is the set of edges, with each edge representing a relation  $r \in \mathcal{R}$ . Our goal is to predict missing relations in the knowledge graph, i.e., given an entity pair  $(h, t)$ , infer the relation  $r$  between them. Specifically, we aim to model the distribution of relation types given the entity pair  $(h, t)$ , denoted as  $p(r|h, t)$ , to capture the complex semantic context and dynamic nature of relations. According to Bayes’ theorem, this distribution can be expressed as:

$$p(r|h, t) \propto p(h, t|r) \cdot p(r), \quad (1)$$

where  $p(r)$  is the prior distribution over relation types, serving as a regularization term. To further model the joint probability  $p(h, t|r)$ ,

we decompose it into a symmetric form:

$$p(h, t|r) = \frac{1}{2} (p(h|r) \cdot p(t|h, r) + p(t|r) \cdot p(h|t, r)). \quad (2)$$

Equation (2) provides guidance for our modeling approach. The terms  $p(h|r)$  and  $p(t|r)$  measure the likelihood of entities  $h$  or  $t$  given the relation  $r$ , reflecting the semantic context of the entities. The terms  $p(t|h, r)$  and  $p(h|t, r)$  capture the dynamic transformation process from  $h$  to  $t$  or from  $t$  to  $h$  given the relation  $r$ , reflecting the dynamic nature of relations. Below, we will illustrate how these two factors are modeled within our approach and how they contribute to relation prediction.

#### 3.2 Flow-Modulated Scoring Model

Figure 2 illustrates the architecture of the Flow-Modulated Scoring model. It consists of two stages: a semantic context learning module and a condition flow-matching module. The first stage encodes context-aware entity embeddings, while the second learns dynamic transformations from head to tail embeddings, generating a context-informed vector field. This field modulates the static score of entity pairs, with the ultimate goal of achieving comprehensive relation prediction. Next, we provide a detailed explanation of these modules.

**3.2.1 Semantic Context Learning Module.** For a given triplet  $(h, r, t)$  in Knowledge Graphs, its semantic context offers valuable cues for identifying valid links from  $h$  to  $t$  [39]. Traditional node-based message passing is applicable to general graphs and has led to numerous variants, such as GCN [12], GraphSAGE [7], and GAT [38]. However, when applied to knowledge graphs, we observe that edges themselves also possess corresponding features (i.e., relation embeddings  $x^e$ ), and the number of relation types is significantly smaller than the number of entities. Modeling message passing over relations is thus more efficient and provides more indicative semantic cues.

To this end, we adopt an improved alternating relational message passing scheme, with its core idea inspired by PathCon [39], and enhance its expressive power by introducing a semantic-aware neighbor selection strategy. Specifically, when generating a message  $m_i^v$  for a node  $v$  by aggregating information from its edges  $\mathcal{E}(v)$ , naively aggregating information from all edges can introduce

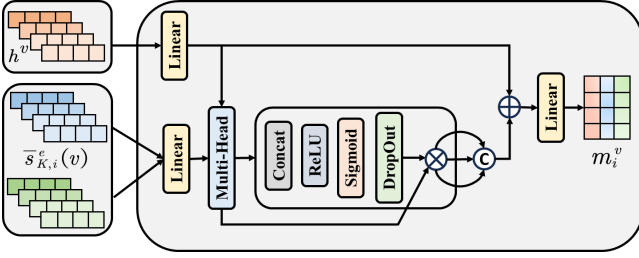


Figure 3: The architecture of attention aggregator.

noise and may lead to information dilution or the over-smoothing problem due to the inclusion of semantically irrelevant edges. To address this challenge, we introduce a **Top-K selection mechanism based on semantic similarity**. Prior to aggregation, we first evaluate the semantic relevance between node  $v$  (represented by its own representation  $h^v$ ) and each of its neighboring edges  $e$  (represented by its current state  $s_i^e$ ). This is achieved by a learnable mapping function  $g(\cdot)$  that projects  $h^v$  and  $s_i^e$  into a shared latent semantic space. In this space, we compute their similarity score using an energy-model inspired scoring function:

$$\text{Score}(v, e) = \exp(-\|g(h^v) - g(s_i^e)\|^2/\tau), \quad (3)$$

where  $\|\cdot\|^2$  is the squared Euclidean distance and  $\tau$  is a temperature hyperparameter. Edges with higher scores, deemed more semantically relevant to node  $v$ , are selected to form the Top-K set  $\mathcal{E}'_K(v) \subseteq \mathcal{E}(v)$ .

The states of these selected Top-K edges,  $\{s_i^e\}_{e \in \mathcal{E}'_K(v)}$ , are first mean-aggregated to form a consolidated neighborhood representation:

$$\bar{s}_{K,i}^e(v) = \text{Mean}(\{s_i^e\}_{e \in \mathcal{E}'_K(v)}). \quad (4)$$

This aggregated edge representation  $\bar{s}_{K,i}^e(v)$ , along with the node's own representation  $h^v$ , is then processed by our specialized node message aggregator. This aggregator (as shown in Figure 3), employs a multi-head attention mechanism. It transforms  $h^v$  and  $\bar{s}_{K,i}^e(v)$ , calculates head-wise gating scores based on their interaction, applies these gates to the transformed  $\bar{s}_{K,i}^e(v)$ , and then combines this gated representation with the transformed  $h^v$  before a final linear projection. This yields a more semantically focused node message  $m_i^v$ :

$$m_i^v = \text{AttentionAggregator}(h^v, \bar{s}_{K,i}^e(v)). \quad (5)$$

The impact of the semantic scoring function and the aggregator selection will be further discussed in subsequent ablation studies.

Next, we generate a message  $m_i^e$  for each edge  $e$ . This message is derived from the node messages  $m_i^v$  and  $m_i^u$  received from its two endpoint nodes  $v$  and  $u$  as follows:

$$m_i^e = \text{MLP}([m_i^v, m_i^u]). \quad (6)$$

Finally, the newly generated edge message  $m_i^e$  is used to update the hidden state of edge  $e$ . The update rule is as follows:

$$s_{i+1}^e = \sigma(\text{Linear}([s_i^e, m_i^e])) \equiv \sigma([s_i^e, m_i^e] \cdot W_i + b_i), \quad (7)$$

where  $\sigma$  is a non-linear activation function,  $[s_i^e, m_i^e]$  represents the concatenation of the previous edge state and the current edge

message, and  $W^i$  and  $b^i$  are the learnable weight matrix and bias term for layer  $i$ , respectively. The initial hidden state of an edge is defined by its intrinsic feature embedding  $s_0^e = x^e \in \mathbb{R}^{d_e}$ .

In this manner, we not only leverage the structure and features of edges in the KG but also, through the semantic-aware neighbor selection mechanism and the subsequent attention-based aggregation, enable the model to more accurately capture and propagate context information most relevant to the specific relation prediction task.

**3.2.2 Condition Flow-Matching Module.** Prior research typically predicts static association scores directly utilizing entity embeddings. Although our Semantic Context Learning module is able to generate more informative entity representations, it is still insufficient to fully characterize the inherent dynamic transformation properties of the relationships. To address this limitation, we have designed the Conditional Flow Matching Module.

The core of this module is learning a dynamic vector field  $v_\theta(t, \mathbf{x})$  that depends on a pseudo-time variable  $t \in [0, 1]$  and the current state  $\mathbf{x} \in \mathbb{R}^d$ . This vector field characterizes the instantaneous direction and velocity along the smooth evolution path of the entity representation, conditioned on a given context  $\mathbf{z}$ , as it transitions from an initial state  $\mathbf{h}$  (i.e., at  $t = 0$ ) to a target state  $\mathbf{t}$  (i.e., at  $t = 1$ ). It is important to note that the variable  $t$  does not represent physical time but rather serves as a pseudo-time dimension parameterizing this transformation process.

Specifically, drawing upon the principles of Conditional Flow Matching [35], we employ a continuous flow to model the transformation from the head entity embedding  $\mathbf{h}^*$  to the tail entity embedding  $\mathbf{t}^*$ . (Note: The asterisk (\*) is used here to distinguish entity representations from the pseudo-time variable  $t$ . This notation will be maintained without repeated clarification). This process can be formalized as:

$$p_t(\mathbf{x}) = \int p_t(\mathbf{x}|\mathbf{z})q(\mathbf{z})d\mathbf{z}, \quad (8)$$

where  $p_t(\mathbf{x})$  represents the marginal probability path,  $q(\mathbf{z})$  is the sampling distribution of the semantic context  $\mathbf{z}$ , and the conditional probability path  $p_t(\mathbf{x}|\mathbf{z})$  denotes the probability path given  $\mathbf{z}$ . Correspondingly, the marginal vector field  $u_t(\mathbf{x})$  that drives the evolution of  $p_t(\mathbf{x})$  can be expressed as an expectation of the conditional vector field  $u_t(\mathbf{x}|\mathbf{z})$  with respect to the prior distribution  $q(\mathbf{z})$ , weighted by the posterior distribution  $p(\mathbf{z}|t, \mathbf{x})$ :

$$u_t(\mathbf{x}) = E_{q(\mathbf{z})} \left[ u_t(\mathbf{x}|\mathbf{z}) \frac{p_t(\mathbf{x})}{p_t(\mathbf{x}|\mathbf{z})} \right], \quad (9)$$

where the conditional vector field is defined as  $u_t(\mathbf{x}|\mathbf{z}) = \frac{d\mathbf{x}}{dt}$ . Consequently, under suitable conditions,  $u_t(\mathbf{x})$  generates the probability flow path  $p_t(\mathbf{x})$ . This formulation allows us to circumvent the need for explicit modeling of the marginal probability path  $p_t(\mathbf{x})$ .

Although we aim to recover  $u_t(\mathbf{x})$ , its direct computation is generally difficult. This is primarily because the computation of  $p_t(\mathbf{x})$  requires integration. Considering the relative tractability of the conditional vector field  $p_t(\mathbf{x}|\mathbf{z})$ , we adopt an indirect learning strategy, and the model is enabled to directly learn an approximation of the vector field  $u_t(\mathbf{x}|\mathbf{z})$ . We assume  $v_\theta : [0, 1] \times \mathbb{R}^d \rightarrow \mathbb{R}^d$  is a time-dependent vector field parameterized by a neural network

with parameters  $\theta$ . We define the following objective function:

$$\mathcal{L}_{cfm}(\theta) = \mathbb{E}_{t,q(z),p_t(x|z)} \|v_\theta(t, \mathbf{x}) - u_t(\mathbf{x}|z)\|_2^2. \quad (10)$$

Based on this, the model learns  $v_\theta(t, \mathbf{x})$ . It can serve as a dynamic adjustment factor to modulate the base static score assigned to the corresponding entity pair. Different choices of  $q(z)$  and  $p_t(x|z)$  determine the different focuses of the model.

In this study, we primarily employ two Conditional Flow Matching paradigms, each based on different assumptions about the underlying dynamics:

**Condition Streaming Matching(CSM)**. This paradigm is grounded in Optimal Transport theory [27] and aims to model the least-cost transformation path from head entity distribution to tail entity distribution. The condition  $\mathbf{z}$  is defined as:  $\mathbf{z} = (\mathbf{h}^*, \mathbf{t}^*)$ . The sampling distribution for the context  $\mathbf{z}$ , denoted as  $q(z)$ :

$$q(z) = \pi(z) = \operatorname{argmin}_{\pi \in \Pi(\rho_H, \rho_T)} \int_{\mathbb{R}^d \times \mathbb{R}^d} \|\mathbf{x} - \mathbf{y}\|_2^2 d\pi(\mathbf{x}, \mathbf{y}), \quad (11)$$

where  $\rho_H$  and  $\rho_T$  represent the marginal distributions of the head and tail entity embeddings, respectively, and  $\Pi(\rho_H, \rho_T)$  is the set of all joint probability distributions. This design aims to guide the model to learn a flow field aligned with the static optimal transport path. In practice, we employ the Minibatch Optimal Transport method for efficient approximation. Thus, the model tends to learn representations that can be transformed into one another with a low transmission cost. We define the conditional probability path and its corresponding conditional vector field as follows:

$$p_t(\mathbf{x}|z) = \mathcal{N}(\mathbf{x} \mid (1-t)\mathbf{h}^* + t\mathbf{t}^*, \sigma^2\mathbf{I}), \quad (12)$$

$$u_t(\mathbf{x}|z) = \mathbf{t}^* - \mathbf{h}^*, \quad (13)$$

where  $p_t(\mathbf{x}|z)$  is a Gaussian distribution, and the noise standard deviation  $\sigma$  controls the stochasticity of the probability path. A moderate value of  $\sigma$  can enhance model robustness. Through CSM, model can learn more direct transformation paths between entities.

**Condition Flow Brownian Bridge Matching(CFBBM)**. This matching paradigm draws upon Schrödinger Bridge theory [28, 34] and aims to model the stochastic evolution process between  $\mathbf{h}^*$  and  $\mathbf{t}^*$ . Its core objective is to find a path probability distribution that is closest to standard Brownian motion, subject to given their distribution constraints.  $\mathbf{z}$  is the same as that in the previous paradigm,  $q(z)$  is designed as an entropy-regularized optimal transport plan:

$$\begin{aligned} q(z) &= \pi_\lambda(z) \\ &= \inf_{\pi \in \Pi(\rho_H, \rho_T)} \int_{\mathbb{R}^d \times \mathbb{R}^d} \|\mathbf{x} - \mathbf{y}\|_2^2 d\pi(\mathbf{x}, \mathbf{y}) - \lambda H(\pi), \end{aligned} \quad (14)$$

where  $\lambda = 2\sigma^2$  and  $H(\pi)$  is the entropy of the joint distribution  $\pi$ . This formulation seeks to minimize the transport cost while simultaneously maximizing entropy (making the transport plan as diffuse as possible), with the trade-off controlled by the regularization parameter  $\lambda$ . With the introduction of entropy regularization, it makes the computation of  $q(z)$  more feasible for large-scale datasets. It can alleviate the high computational complexity of the previous paradigm. Under this paradigm, the conditional probability path and its corresponding conditional vector field are defined as follows:

$$p_t(\mathbf{x}|z) = \mathcal{N}(\mathbf{x} \mid (1-t)\mathbf{t}^* + t\mathbf{h}^*, t(1-t)\sigma^2\mathbf{I}), \quad (15)$$

$$u_t(\mathbf{x}|z) = \frac{1-2t}{2t(1-t)} (\mathbf{x} - ((1-t)\mathbf{t}^* + t\mathbf{h}^*)) + (\mathbf{h}^* - \mathbf{t}^*), \quad (16)$$

where  $t(1-t)\sigma^2\mathbf{I}$  reflects the characteristic diffusion properties of a Brownian bridge process. Through this matching strategy, the model is guided to learn a dynamic flow field that simulates the stochastic evolutionary path connecting the embeddings of two entities. This facilitates the capture of potentially more complex and non-linear stochastic evolutionary relationships between entities.

**3.2.3 Module Integration and Overall Scoring Process.** In this section, we will detail how the two aforementioned modules are integrated to achieve comprehensive relation prediction.

Firstly, we utilize the Semantic Context Learning module to compute the final messages  $m_{j-1}^h$  and  $m_{j-1}^t$  for the head entity  $h$  and the tail entity  $t$ . These messages summarize their respective consistent contextual semantics. Subsequently, we represent the static score for the entity pair  $(h, t)$  as follows:

$$s_{(h,t)} = \sigma \left( \left[ m_{j-1}^h, m_{j-1}^t \right] \cdot W_{j-1} + b_{j-1} \right). \quad (17)$$

Note that Equation (17) should only take the messages of  $h$  and  $t$  as input, without including their connecting edge  $r$ , since the ground-truth relation  $r$  is treated as unobserved during the training stage.

Secondly, we employ the Condition Flow-Matching Module. Given the contextual condition  $\mathbf{z} = (m_{j-1}^h, m_{j-1}^t) = (\mathbf{h}^*, \mathbf{t}^*)$ , where the second symbol representation used here for the CFM module is for the sake of convenience in representation, this module predicts a dynamic vector field  $v_\theta(t, \mathbf{x})$ . This vector field characterizes the instantaneous velocity and direction of the transformation from an initial state  $\mathbf{h}^*$  (i.e.,  $\mathbf{x}$  at  $t = 0$ ) to a target state  $\mathbf{t}^*$  (i.e.,  $\mathbf{x}$  at  $t = 1$ ). We then use this vector field to dynamically modulate the basic static score of the entity pair as follows:

$$s_{(h,t)} = s_{(h,t)} \odot v_\theta(t, \mathbf{x}). \quad (18)$$

Given the flow-modulated score of the entity pair  $s_{(h,t)}$ , we can convert the score into a probability distribution over relations by applying softmax, which then allows us to predict the relations:

$$p(r|h, t) = \operatorname{SoftMax} \left( s_{(h,t)} \right). \quad (19)$$

The primary objective for relation prediction is to minimize the loss between the predicted probabilities and the ground-truth relations over the training triplets  $\mathcal{D}$ :

$$\mathcal{L}_{pred}(\Phi_S, \theta) = \sum_{(h,r,t) \in \mathcal{D}} J(p(r|h, t), r), \quad (20)$$

where  $J(\cdot)$  is the cross-entropy loss function, and  $\Phi_S$  represents all learnable parameters of the Semantic Context Learning module and the static scoring Linear.

To train the entire model effectively, we adopt a joint training strategy. The overall loss function  $\mathcal{L}$  combines the relation prediction loss with the Condition Flow-Matching loss. The Condition Flow-Matching loss ensures that the learned vector field  $v_\theta(t, \mathbf{x})$  accurately approximates the desired conditional dynamics. The final training objective is to minimize the weighted sum of these losses:

$$\mathcal{L}(\Phi_S, \theta) = \mathcal{L}_{pred}(\Phi_S, \theta) + \lambda \mathcal{L}_{cfm}(\theta), \quad (21)$$

---

**Algorithm 1** FMS Training Process

---

- 1: **Input:** Batch data  $(h, t)$  and  $r$ , where  $(h, t)$  are entity pairs,  $r$  are relation labels.
  - 2: **Parameters:** Relation embeddings, Semantic Context Learning Module, MLP, Linear.
  - 3: **repeat**
  - 4:    $\mathbf{h}^* = \text{Semantic Context Learning Module}(h)$ ;
  - 5:    $\mathbf{t}^* = \text{Semantic Context Learning Module}(t)$ ;
  - 6:    $t, x_t, u_t \sim \text{Condition Flow-Matching Module}(\mathbf{h}^*, \mathbf{t}^*)$ ;
  - 7:    $v_\theta(t, \mathbf{x}) = \text{MLP}([x_t, t])$ ;
  - 8:    $s_{(h,t)} = \text{Linear}([\mathbf{h}^*, \mathbf{t}^*])$ ;
  - 9:    $s_{(h,t)} = s_{(h,t)} \odot v_\theta(t, \mathbf{x})$ ;
  - 10:    $\mathcal{L}_{cfm}(\theta) = \mathbb{E}_{t,q(z),p_t(x|z)} \|v_\theta(t, \mathbf{x}) - u_t(\mathbf{x}|z)\|_2^2$ ;
  - 11:    $\mathcal{L}_{pred}(\Phi_S, \theta) = \sum_{(h,r,t) \in \mathcal{D}} J(p(r|h, t), r)$ ;
  - 12:    $\mathcal{L}(\Phi_S, \theta) = \mathcal{L}_{pred}(\Phi_S, \theta) + \lambda \mathcal{L}_{cfm}(\theta)$ ;
  - 13:   Update model parameters using gradient descent on  $\mathcal{L}$ .
  - 14: **until** converged
- 

where  $\lambda$  is a hyperparameter that balances the contribution of the two loss terms. The training process of FMS are illustrated in Algorithm 1.

It is worth noticing that the initial context representation derived from  $\mathbf{h}^*$  and  $\mathbf{t}^*$  plays a dual role: it directly contributes to the base score for relation prediction, and it also serves as the condition  $\mathbf{z}$  for the flow-matching module, thereby influencing the dynamic modulation factor.

## 4 Experiment

To evaluate the effectiveness of our FMS, we have designed a series of experiments to address the following research questions:

- **RQ1:** How does the performance of FMS compare to a diverse range of mainstream prediction models?
- **RQ2:** What distinct contributions do the key components of FMS offer to the overall performance? Additionally, how does the model’s performance adapt and respond to variations in hyperparameter settings?
- **RQ3:** How does FMS perform in terms of its number of parameters?
- **RQ4:** How does FMS modulate the static scores of triplets to capture the dynamic nature of relations?

### 4.1 Transductive Experiment Settings

**Datasets.** We conduct experiments on six knowledge graph datasets: (i) FB15K, derived from Freebase, a large-scale KG of general human knowledge; (ii) FB15K-237, a subset of FB15K where inverse relations are removed; (iii) WN18, containing conceptual-semantic and lexical relations among English words from WordNet; (iv) WN18RR, a subset of WN18 where inverse relations are removed; (v) NELL995, extracted from the 995th iteration of the NELL system, containing general knowledge; (vi) DDB14, collected from Disease Database, a medical database containing terminologies, concepts (diseases, symptoms, drugs), and their relationships. The statistics above are summarized in Table 1.

**Table 1: Statistics of all datasets.  $\mathbb{E}[d]$  and  $\text{Var}[d]$  are mean and variance of the node degree distribution, respectively.**

Datasets	Nodes	Relations	Train	Val	Test	$\mathbb{E}[d]$	$\text{Var}[d]$
FB15K	15.0k	1.3k	483.1k	50.0k	59.1k	64.6	32.4k
FB15K-237	14.5k	237	272.1k	17.5k	20.5k	37.4	12.3k
WN18	40.9k	18	141.4k	5.0k	5.0k	6.9	236.4
WN18RR	40.9k	11	86.8k	3.0k	3.1k	4.2	64.3
NELL995	63.9k	198	137.5k	5.0k	5.0k	4.3	750.6
DDB14	9.2k	14	36.6k	4.0k	4.0k	7.9	978.8

**Baselines.** Based on the concept of Knowledge Graph Completion, we categorize all baseline methods into four groups: **(i) Emb-based:** TransE [2], ComplEx [36], DistMult [42], RotatE [31], SimpleE [11], QuatE [45]; **(ii) Rule-based:** DRUM [25], and PTransE [23]; **(iii) GNN-Based:** R-GCN [26], Pathcon [39], and LASS [29] **(iv) LLM-Based:** KG-BERT [44], KGE-BERT [20], and GilBERT [21]

**Evaluation Metrics.** For each test triplet  $(h, r, t)$ , we construct the queries:  $(h, ?, t)$ <sup>1</sup>, where the answers are  $r$ . Analogous to the evaluation method employed in link prediction, the mean Reciprocal Rank (MRR) and Hits@N are selected as evaluation metrics, with definitions consistent with previous research. Higher MRR and H@N scores signify superior model efficacy.

### 4.2 Inductive Experiment Settings

**Datasets.** Following [46], we utilize a total of twelve subsets, encompassing four distinct versions each, which are derived from established datasets: WN18RR, FB15k237, and NELL-995. Each subset is uniquely characterized by a disparate split between the training and test sets, ensuring a robust and comprehensive evaluation schema. For a detailed discourse on the specific splits and a nuanced presentation of the statistical attributes of each subset, one can refer to the comprehensive descriptions available in [46].

**Baselines.** For inductive learning, traditional Embedding-based methods are not suitable for the task due to their inability to generalize to unseen entities, we choose the following two classes of classical and effective models: **(i) Rule-based:** RuleN [19], NeuralLP [43], DRUM [25]; **(ii) GNN-based:** GraIL [33], PathCon [39].

**Evaluation Metrics.** The setup and parameter selection are consistent with the transduction experiments.

### 4.3 Overall Performance Comparison: RQ1

To answer RQ1, we conducted extensive experiments comparing FMS with the strongest baseline we know of, both in terms of transductive and inductive learning.

<sup>1</sup>Some related work formulates this as predicting missing tail (or head) entities given a head (or tail) entity and a relation. These two problems (entity prediction and relation prediction) are reducible to each other. For instance, a relation prediction model  $\Phi(\cdot|h, t)$  can be converted to a tail prediction model  $\Gamma(\cdot|h, r) = \text{SoftMax}_t(\Phi(r|h, t))$ , and vice versa. Given this equivalence, this work focuses on relation prediction.

Table 2: Transductive performance comparison on all six datasets. The results here are expressed as percentages. The best results are shown in bold while the second-best results are shown in the underline.

Type	Model	FB15K			FB15K-237			WN18			WN18RR			NELL995			DDB14		
		MRR	H@1	H@3															
Emb-based	TransE	96.2	94.0	98.2	96.6	94.6	98.4	97.1	95.5	98.4	78.4	66.9	87.0	84.1	78.1	88.9	96.6	94.8	98.0
	ComplEx	90.1	84.4	95.2	92.4	87.9	97.0	98.5	97.9	99.1	84.0	77.7	88.0	70.3	62.5	76.5	95.3	93.1	96.8
	DistMult	66.1	43.9	86.8	87.5	80.6	93.6	78.6	58.4	98.7	84.7	78.7	89.1	63.4	52.4	72.0	92.7	88.6	96.1
	RotatE	97.9	96.7	98.6	97.0	95.1	98.0	98.4	97.9	98.6	79.9	73.5	82.3	72.9	69.1	75.6	95.3	93.4	96.4
	Simple	98.3	97.2	99.1	97.1	95.5	98.7	97.2	96.4	97.6	73.0	65.9	75.5	71.6	67.1	74.8	92.4	89.2	94.8
	QuatE	98.3	97.2	99.1	97.4	95.8	98.8	98.1	97.5	98.3	82.3	76.7	85.2	75.2	70.6	78.3	94.6	92.2	96.2
Rule-based	DRUM	94.5	94.5	97.8	95.9	90.5	95.8	96.9	95.6	98.0	85.4	77.8	91.2	71.5	64.0	74.0	95.8	93.0	98.7
	PTransE	-	-	-	96.2	96.0	98.5	98.7	98.2	98.9	85.3	87.5	94.7	-	-	-	-	-	-
GNN-based	R-GCN	-	-	-	93.1	90.3	94.2	90.9	82.4	97.9	82.2	75.0	84.8	-	-	-	-	-	-
	Pathcon	<u>98.4</u>	<u>97.4</u>	<u>99.5</u>	<u>97.9</u>	<u>96.4</u>	<u>99.4</u>	<u>99.3</u>	<u>98.8</u>	<u>99.8</u>	<u>97.4</u>	<u>95.4</u>	<u>99.4</u>	<u>89.6</u>	<u>84.4</u>	<u>94.1</u>	<u>98.0</u>	<u>96.6</u>	<u>99.5</u>
	LASS	-	-	-	97.3	95.5	98.8	96.7	95.9	98.0	95.9	94.2	96.4	-	-	-	-	-	-
LLM-based	KG-BERT	-	-	-	97.3	95.2	98.6	96.7	94.6	98.2	94.2	91.7	96.8	-	-	-	-	-	-
	KGE-BERT	-	-	-	97.2	94.3	99.0	96.5	95.7	97.9	94.8	92.4	96.1	-	-	-	-	-	-
	GilBERT	-	-	-	95.1	91.4	97.0	96.5	94.7	98.1	94.1	91.6	96.7	-	-	-	-	-	-
Ours	FMS	<b>99.6</b>	<b>99.5</b>	<b>99.8</b>	<b>99.8</b>	<b>99.7</b>	<b>99.9</b>	<b>99.7</b>	<b>99.5</b>	<b>99.9</b>	<b>99.9</b>	<b>99.8</b>	<b>99.9</b>	<b>99.1</b>	<b>98.6</b>	<b>99.5</b>	<b>99.8</b>	<b>99.7</b>	<b>99.9</b>

Table 3: Inductive results (Hits@10). The best results are shown in bold while the second-best results are shown underlined.

Type	Model	WN18RR				FB15k-237				NELL-995			
		v1	v2	v3	v4	v1	v2	v3	v4	v1	v2	v3	v4
Rule-based	Neural-LP	74.4	68.9	46.2	67.1	52.9	58.9	52.9	55.9	40.8	78.7	82.7	80.6
	DRUM	74.4	68.9	46.2	67.1	52.9	58.7	52.9	55.9	19.4	78.6	82.7	80.6
	RuleN	80.9	78.2	53.4	71.6	49.8	77.8	87.7	85.6	<u>53.5</u>	81.8	77.3	61.4
GNN-based	GraLL	82.5	78.7	58.4	73.4	64.2	81.8	82.8	89.3	<b>59.5</b>	93.3	91.4	73.2
	PathCon	<u>97.6</u>	<u>97.1</u>	<u>97.4</u>	<u>98.7</u>	<u>94.1</u>	<u>95.6</u>	<u>95.9</u>	<u>96.0</u>	-	<u>95.8</u>	<u>94.5</u>	<u>95.6</u>
Ours	FMS	<b>99.2</b>	<b>98.4</b>	<b>99.0</b>	<b>99.5</b>	<b>98.4</b>	<b>99.5</b>	<b>99.6</b>	<b>99.9</b>	-	<b>99.5</b>	<b>99.2</b>	<b>99.8</b>

Table 4: Results by relation category on FB15k-237.

Model	1-1		1-N	
	MRR	Hit@1	MRR	Hit@1
PathCon	92.4	88.9	80.9	74.2
FMS	<b>99.8</b>	<b>99.7</b>	<b>99.6</b>	<b>99.3</b>

Table 5: Ablation study on key components of FMS.

Ablation Settings	FB15k-237		WN18RR	
	MRR	Hit@1	MRR	Hit@1
FMS	<b>99.8</b>	<b>99.7</b>	<b>99.9</b>	<b>99.8</b>
FMS w/o Top-K	97.8	96.1	94.3	89.4
FMS w/o Score	98.2	97.1	97.4	95.9
FMS w/o Flow-Matching	98.7	97.9	98.4	97.5

The transductive results are summarized in Table 2. FMS shows remarkable improvement across all metrics on six datasets. Specifically, FMS achieves a **1.2% relative**, **1.7% relative**, **0.4% relative**, **2.5% relative**, **10.6% relative**, and **1.8% relative** increase in MRR scores over the best baselines on FB15K, FB15k-237, WN18, WN18RR, NELL995, and DDB14, respectively. These consistent and significant gains across diverse datasets, particularly the substantial improvement on NELL995, underscore the robustness and superior capability of our proposed FMS model. Furthermore, it is important

to note that, compared to all kinds of models, FMS achieves better results for MRR scores on all datasets, establishing its state-of-the-art performance.

To further analyze the performance of FMS, we decomposed FB15k-237 based on relation categories similar to those defined in [41]. We redefined the 1-N task by specifically isolating a test subset where each entity pair has two or more relation types. As

**Table 6: Number of parameters of all models on DDB14.**

Model	TransE	DisMult	RotatE	QuatE	PathCon	FMS
Param	3.7M	3.7M	7.4M	14.7M	0.06M	<b>0.02M</b>

**Table 7: Number of parameters of all models on FB15k-237.**

Model	TransE	DisMult	RotatE	QuatE	PathCon	FMS
Param	5.9M	5.9M	11.7M	23.6M	1.67M	<b>0.35M</b>

shown in Table 4, FMS achieved overwhelmingly superior performance, indicating its successful capture of the dynamic nature of relations.

The inductive results are summarized in Table 3. FMS shows remarkable improvement across Hits@10 metrics on twelve datasets. It is noteworthy that while the optimal performance of other models typically ranges between 70% and 90% except PathCon, the FMS model almost consistently achieves between 98% and 99.9%, demonstrating its overwhelming advantage in inductive learning capabilities. Furthermore, FMS maintains near-perfect performance across different versions and splits of various datasets, indicating that the model possesses excellent stability and robustness to data variations.

#### 4.4 Ablation Study: RQ2

**4.4.1 Key Modules Ablation Study.** To verify the effectiveness of our proposed modules, we develop three distinct model variants:

- **w/o Top-K:** We replace the Top-K selection mechanism based on semantic similarity in the Semantic Context Learning Module with a simple random sampling strategy.
- **w/o Score:** We remove the energy-model inspired scoring function, and instead use dot product similarity for scoring.
- **w/o Flow-Matching:** We remove the Condition Flow-Matching Module, relying solely on the basic static scores of entity pairs.

The ablation study results are presented in Table 5, leading to the following key conclusions: The Top-K selection mechanism exerts the most significant impact on the overall FMS performance, with its absence leading to a substantial decline in performance, particularly on the WN18RR dataset. This underscores Top-K’s pivotal role in filtering critical information and suppressing noise. Secondly, the energy-model inspired scoring function is also crucial for evaluating and ranking candidate answers, and its removal results in a noticeable loss in performance. While the Condition Flow-Matching Module has a comparatively smaller impact, it still provides a stable performance gain for the model. Therefore, the synergistic interaction of these components is a key factor enabling the FMS model to maintain its state-of-the-art performance.

**4.4.2 Sensitivity to Key Hyperparameters.** In this study, we analyze the impact of key hyperparameters within the Semantic Context Learning Module and the effect of different aggregator choices. The results on the FB15k-237 dataset are presented in Figure 4.

Figure 4(a) shows how FMS performance varies with different Top-K values. The results demonstrate that a moderate K value (specifically 10 in this case) is critical. An overly small K provides insufficient context to leverage, while an excessively large K introduces increasing noise, potentially overwhelming the model with excessive contextual information and causing a drop in performance.

Figure 4(b) then shows the performance of FMS’s Semantic Context Learning Module when using different context aggregators. It can be seen that our designed self-attention aggregator performs best, while the mean aggregator performs worst.

Figure 4(c) illustrates the selection of hop count on the graph. The results indicate that FMS achieves competitive performance at the first hop and optimal performance at the second hop. Further increasing the hop count, however, leads to performance degradation. This phenomenon is likely attributable to the exponential increase in neighbor sampling associated with deeper hops, which consequently introduces more noise. Nevertheless, owing to the mechanisms of Top-k selection and attention aggregation, the model maintains its state-of-the-art performance.

#### 4.5 Efficiency Analysis: RQ3

We performed parametric volume analysis on both datasets, on the smaller dataset DDB14 as in Table 6 and on the larger dataset FB15k-237 as in Table 7. The model complexity is  $O(n \cdot K^{Hops})$ . The result demonstrates that FMS is much more storage-efficient than embedding-based methods, since it does not need to calculate and store entity embeddings. Furthermore, FMS is significantly more effective than GNN-based methods such as PathCon. FMS can achieve superior performance with fewer hops and a smaller number of sampled neighbors. Additionally, it does not require explicitly modeling paths from the head entity to the tail entity like PathCon; instead, it employs flow-matching to learn a dynamic transition vector field, which represents semantically context-guided paths.

#### 4.6 Case Study: RQ4

To quantitatively evaluate the impact of the Flow-Modulated Scoring (FMS) framework, we investigate using an example from the FB15k-237 dataset. The task is defined as: (California College of the Arts, ?, United States Dollar), for which the correct relations are: Revenue Currency, Operating Income Currency, Local Tuition Currency, Assets Currency, Domestic Tuition Currency, and Endowment Currency. Figure 5 presents T-SNE [37] visualizations to compare the representations learned by FMS against those from traditional static scoring methods.

Central to the figure, the "Static Score Embedding" (black square) represents the generalized initial understanding that a traditional static model might offer for the association between "California College of the Arts" and "United States Dollar." Due to its singular nature, this single point struggles to simultaneously and precisely encapsulate the specific role of "United States Dollar" as a currency across six different financial contexts. The power of FMS is evident in its subsequent dynamic processing. Observing the 'Dynamic Scores' (colored stars) in the figure, we see that FMS is not content with this single, potentially ambiguous static representation. Instead, it actively transforms or "flows" from this static starting point

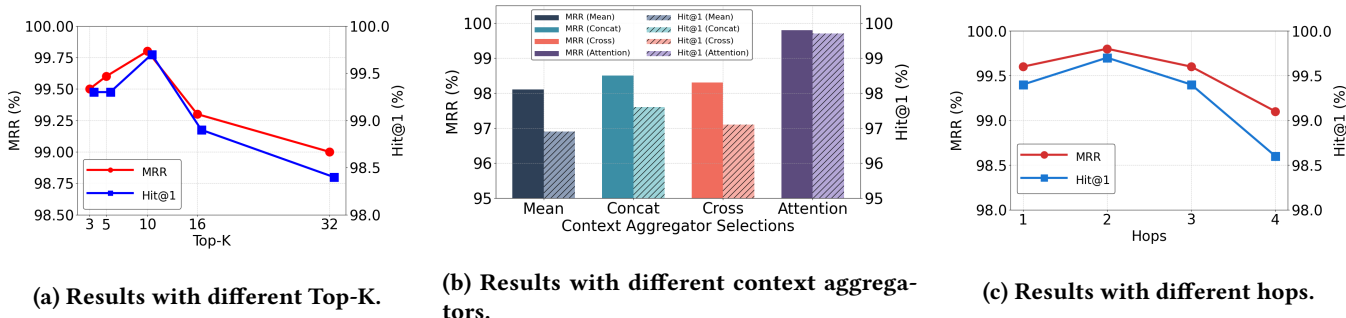


Figure 4: Hyper-parameters analysis of FMS on FB15k-237.

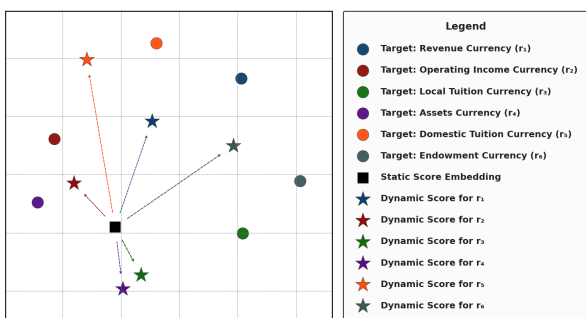


Figure 5: T-SNE visualization of Static Score versus Flow-Modulated Score representations on FB15k-237.

to generate specific embedding representations for each potential relation. Each arrow in the figure symbolizes this context-driven modulation process, guiding the initial representation towards more relevant and fine-grained semantic space regions associated with specific relation types.

FMS successfully distinguishes between multiple concurrently valid relations. It does not merely identify the generic concept of “currency”; rather, it can precisely differentiate specific relations such as “Revenue Currency” and “Assets Currency” within the embedding space. This clearly demonstrates its exceptional performance in capturing the dynamic nature of knowledge graph relations.

## 5 Conclusion

In this work, we introduced Flow-Modulated Scoring (FMS), a novel framework designed to address the limitations of existing knowledge graph completion methods in modeling multifaceted semantic relationships and their dynamic nature. FMS innovatively combines a semantic context learning module, which generates context-aware entity embeddings, with a condition flow-matching module that learns the transformation dynamics between entities based on this context. By using the predicted vector field to dynamically modulate a base static score, FMS effectively synergizes rich static representations with conditioned dynamic flow information.

Our comprehensive experiments on several well-established benchmarks demonstrate that FMS achieves state-of-the-art performance, validating its capability to capture more comprehensive relational semantics and advance the field of relation prediction.

## 6 GenAI Usage Disclosure

We confirm that no generative AI software was used to create any of the above content, including charts, code, and data. Any such AI tools were used solely to refine spelling, grammar, and translation to improve the readability of the paper.

## References

- [1] Michael S. Albergo and Eric Vanden-Eijnden. 2023. Building normalizing flows with stochastic interpolants. In *International Conference on Learning Representations (ICLR)*.
- [2] Antoine Bordes, Nicolas Usunier, Alberto Garcia-Duran, Jason Weston, and Oksana Yakhnenko. 2013. Translating embeddings for modeling multi-relational data. *Advances in neural information processing systems* 26 (2013).
- [3] Nanxin Chen, Yu Zhang, Heiga Zen, Ron J Weiss, Mohammad Norouzi, and William Chan. 2020. Wavegrad: Estimating gradients for waveform generation. *arXiv preprint arXiv:2009.00713* (2020).
- [4] Ricky T.Q. Chen and Yaron Lipman. 2024. Flow matching on general geometries. In *International Conference on Learning Representations (ICLR)*.
- [5] Ricky TQ Chen, Yulia Rubanova, Jesse Bettencourt, and David K Duvenaud. 2018. Neural ordinary differential equations. *Advances in neural information processing systems* 31 (2018).
- [6] Tim Dettmers, Pasquale Minervini, Pontus Stenetorp, and Sebastian Riedel. 2018. Convolutional 2d knowledge graph embeddings. In *Proceedings of the AAAI Conference on Artificial Intelligence (AAAI)*, Vol. 32.
- [7] Will Hamilton, Zhitaoying, and Jure Leskovec. 2017. Inductive representation learning on large graphs. *Advances in neural information processing systems* 30 (2017).
- [8] Jonathan Ho, Ajay Jain, and Pieter Abbeel. 2020. Denoising diffusion probabilistic models. *Advances in neural information processing systems* 33 (2020), 6840–6851.
- [9] Aidan Hogan, Eva Blomqvist, Michael Cochez, Claudia d’Amato, Gerard de Melo, Claudio Gutierrez, Sabrina Kirrane, José Emilio Labra Gayo, Roberto Navigli, Sebastian Neumaier, et al. 2021. Knowledge graphs. *ACM Computing Surveys (CSUR)* 54, 4 (2021), 1–37.
- [10] Guoliang Ji, Shizhu He, Liheng Xu, Kang Liu, and Jun Zhao. 2015. Knowledge graph embedding via dynamic mapping matrix. In *Proceedings of the 53rd Annual Meeting of the Association for Computational Linguistics and the 7th International Joint Conference on Natural Language Processing (ACL-IJCNLP)*. 687–696.
- [11] Seyed Mehran Kazemi and David Poole. 2018. Simple embedding for link prediction in knowledge graphs. *Advances in neural information processing systems* 31 (2018).
- [12] Thomas N Kipf and Max Welling. 2016. Semi-supervised classification with graph convolutional networks. *arXiv preprint arXiv:1609.02907* (2016).
- [13] Zhifeng Kong, Wei Ping, Jiayi Huang, Kexin Zhao, and Bryan Catanzaro. 2020. Diffwave: A versatile diffusion model for audio synthesis. *arXiv preprint arXiv:2009.09761* (2020).
- [14] Haoying Li, Yifan Yang, Meng Chang, Shiqi Chen, Huajun Feng, Zhihai Xu, Qi Li, and Yueting Chen. 2022. Srdiff: Single image super-resolution with diffusion probabilistic models. *Neurocomputing* 479 (2022), 47–59.

- [15] Xiang Li, John Thickstun, Ishaan Gulrajani, Percy S Liang, and Tatsunori B Hashimoto. 2022. Diffusion-lm improves controllable text generation. *Advances in Neural Information Processing Systems* 35 (2022), 4328–4343.
- [16] Yankai Lin, Zhiyuan Liu, Maosong Sun, Yang Liu, and Xuan Zhu. 2015. Learning entity and relation embeddings for knowledge graph completion. In *Proceedings of the AAAI Conference on Artificial Intelligence (AAAI)*, Vol. 29.
- [17] Yaron Lipman, Ricky T.Q. Chen, Heli Ben-Hamu, Maximilian Nickel, and Matt Le. 2023. Flow matching for generative modeling. In *International Conference on Learning Representations (ICLR)*.
- [18] Qiang Liu. 2022. Rectified flow: A marginal preserving approach to optimal transport. *arXiv preprint arXiv:2209.14577* (2022).
- [19] Christian Meilicke, Manuel Fink, Yanjie Wang, Daniel Ruffinelli, Rainer Gemulla, and Heiner Stuckenschmidt. 2018. Fine-grained evaluation of rule-and embedding-based systems for knowledge graph completion. In *The semantic web—ISWC 2018: 17th international semantic web conference, Monterey, CA, USA, October 8–12, 2018, proceedings, part I 17*. Springer, 3–20.
- [20] Rahul Nadkarni, David Wadden, Iz Beltagy, Noah A Smith, Hannaneh Hajishirzi, and Tom Hope. 2021. Scientific language models for biomedical knowledge base completion: An empirical study. *arXiv preprint arXiv:2106.09700* (2021).
- [21] Armita Khajeh Nassiri, Nathalie Pernelle, Fatiha Saïs, and Gianluca Quercini. 2022. Knowledge Graph Refinement based on Triplet BERT-Networks. *arXiv preprint arXiv:2211.10460* (2022).
- [22] David N Nicholson and Casey S Greene. 2020. Constructing knowledge graphs and their biomedical applications. *Computational and Structural Biotechnology Journal* 18 (2020), 1414–1428.
- [23] Zhihan Peng, Hong Yu, and Xiuyi Jia. 2022. Path-based reasoning with K-nearest neighbor and position embedding for knowledge graph completion. *Journal of Intelligent Information Systems* (2022), 1–21.
- [24] Aram-Alexandre Pooladian, Heli Ben-Hamu, Carles Domingo-Enrich, Brandon Amos, Yaron Lipman, and Ricky T.Q. Chen. 2023. Multisample flow matching: Straightening flows with minibatch couplings. In *International Conference on Learning Representations (ICLR)*.
- [25] Ali Sadeghian, Mohammadreza Armandpour, Patrick Ding, and Daisy Zhe Wang. 2019. Drum: End-to-end differentiable rule mining on knowledge graphs. *Advances in neural information processing systems* 32 (2019).
- [26] Michael Schlichtkrull, Thomas N. Kipf, Peter Bloem, Rianne van den Berg, Ivan Titov, and Max Welling. 2018. Modeling Relational Data with Graph Convolutional Networks. *The Semantic Web* 10843 (2018), 593–607. doi:10.1007/978-3-319-93417-4\_38
- [27] Alexander Schrijver. 2003. *Combinatorial Optimization*. Springer, Berlin; New York. See p. 362.
- [28] Erwin Schrödinger. 1932. Sur la théorie relativiste de l'électron et l'interprétation de la mécanique quantique. *Annales de l'institut Henri Poincaré* 2, 4 (1932), 269–310.
- [29] Jianhao Shen, Chenguang Wang, Linyuan Gong, and Dawn Song. 2022. Joint language semantic and structure embedding for knowledge graph completion. *arXiv preprint arXiv:2209.08721* (2022).
- [30] Yang Song, Jascha Sohl-Dickstein, Diederik P Kingma, Abhishek Kumar, Stefano Ermon, and Ben Poole. 2020. Score-based generative modeling through stochastic differential equations. *arXiv preprint arXiv:2011.13456* (2020).
- [31] Zhiqing Sun, Zhi-Hong Deng, Jian-Yun Nie, and Jian Tang. 2019. Rotate: Knowledge graph embedding by relational rotation in complex space. *arXiv preprint arXiv:1902.10197* (2019).
- [32] Yusuke Tashiro, Jiaming Song, Yang Song, and Stefano Ermon. 2021. Csd: Conditional score-based diffusion models for probabilistic time series imputation. *Advances in Neural Information Processing Systems* 34 (2021), 24804–24816.
- [33] Komal Teru, Etienne Denis, and Will Hamilton. 2020. Inductive relation prediction by subgraph reasoning. In *International conference on machine learning*. PMLR, 9448–9457.
- [34] Alexander Tong, Kilian Fatras, Nikolay Malkin, Guillaume Hugué, Yanlei Zhang, Jarrid Rector-Brooks, Guy Wolf, and Yoshua Bengio. 2023. Improving and generalizing flow-based generative models with minibatch optimal transport. arXiv:2302.00482 [cs.LG] <https://arxiv.org/abs/2302.00482>
- [35] Alexander Tong, Kilian Fatras, Nikolay Malkin, Guillaume Hugué, Yanlei Zhang, Jarrid Rector-Brooks, Guy Wolf, and Yoshua Bengio. 2023. Improving and Generalizing Flow-Based Generative Models with Minibatch Optimal Transport. *Transactions on Machine Learning Research* (2023). doi:10.48550/arXiv.2302.00482 arXiv:2302.00482 [cs.LG]
- [36] Théo Trouillon, Johannes Welbl, Sebastian Riedel, Éric Gaussier, and Guillaume Cevaert. 2016. Complex embeddings for simple link prediction. In *Proceedings of the 33rd International Conference on Machine Learning (ICML)*. 2071–2080.
- [37] Laurens Van der Maaten and Geoffrey Hinton. 2008. Visualizing data using t-SNE. *Journal of machine learning research* 9, Nov (2008), 2579–2605.
- [38] A Vaswani. 2017. Attention is all you need. *Advances in Neural Information Processing Systems* (2017).
- [39] Hongwei Wang, Hongyu Ren, and Jure Leskovec. 2021. Relational message passing for knowledge graph completion. In *Proceedings of the 27th ACM SIGKDD Conference on Knowledge Discovery & Data Mining*. 1697–1707.
- [40] Quan Wang, Zhen Dong Mao, Bin Wang, and Li Guo. 2017. Knowledge graph embedding: A survey of approaches and applications. *IEEE Transactions on Knowledge and Data Engineering* 29, 12 (2017), 2724–2743.
- [41] Zhen Wang, Jianwen Zhang, Jianlin Feng, and Zheng Chen. 2014. Knowledge graph embedding by translating on hyperplanes. In *Proceedings of the AAAI Conference on Artificial Intelligence (AAAI)*, Vol. 28.
- [42] Bishan Yang, Wen-tau Yih, Xiaodong He, Jianfeng Gao, and Li Deng. 2015. Embedding entities and relations for learning and inference in knowledge bases. In *International Conference on Learning Representations (ICLR)*.
- [43] Fan Yang, Zhilin Yang, and William W Cohen. 2017. Differentiable learning of logical rules for knowledge base reasoning. *Advances in neural information processing systems* 30 (2017).
- [44] Liang Yao, Chengsheng Mao, and Yuan Luo. 2019. KG-BERT: BERT for knowledge graph completion. *arXiv preprint arXiv:1909.03193* (2019).
- [45] Shuai Zhang, Yi Tay, Lina Yao, and Qi Liu. 2019. Quaternion knowledge graph embeddings. *Advances in neural information processing systems* 32 (2019).
- [46] Yongqi Zhang and Quanming Yao. 2022. Knowledge graph reasoning with relational digraph. In *Proceedings of the ACM web conference 2022*. 912–924.